Published in final edited form as:

J Neurosurg. 2018 March ; 128(3): 875–884. doi:10.3171/2016.11.JNS16976.

Noninvasive neuromodulation and brain mapping with low intensity focused ultrasound

Robert F. Dallapiazza, MD PhD[1], **Kelsie F. Timbie, BS**[2], **Stephen Holmberg, CINM**[6], **Jeremy Gatesman, BA LVT**[3], **M. Beatriz Lopes, MD PhD**[4], **Richard J. Price, PhD**[2], **G. Wilson Miller, PhD**[5], **W. Jeffrey Elias, MD**[1]

[1]Department of Neurosurgery, University of Virginia, Charlottesville, Virginia

[2]Department of Biomedical Engineering, University of Virginia, Charlottesville, Virginia

[3]Department of Comparative Medicine, University of Virginia, Charlottesville, Virginia

[4]Department of Pathology (Neuropathology), University of Virginia, Charlottesville, Virginia

[5]Department of Radiology, University of Virginia, Charlottesville, Virginia

[6]Department of Impulse Monitoring, University of Virginia, Charlottesville, Virginia

Abstract

Object: Ultrasound can be precisely focused through the intact human skull to target deep regions of the brain. Since acoustic energy is capable of both exciting and inhibiting neural tissues, transcranial focused ultrasound could potentially be used to noninvasively map the brain.

Methods: The swine sensory thalamus was stereotactically targeted with low intensity focused ultrasound, and somatosensory evoked potentials were recorded from an epidural grid electrode. Magnetic resonance thermography was used to assess tissue heating at the acoustic focus and tissue was assessed histologically for damage.

Results: Low intensity focused ultrasound inhibited sensory evoked potentials with a spatial resolution ~2mm. This method could be used to selectively inhibit adjacent thalamic nuclei. The ventromedial thalamic nucleus could be inhibited without effecting the ventrolateral nucleus. There was no observed tissue heating during sonications and no histological evidence of tissue damage.

Conclusions: These results suggest that low intensity focused ultrasound can be safely used to modulate neuronal circuits in the central nervous system and that noninvasive brain mapping with focused ultrasound is feasible for use in humans.

Keywords

Neuromodulation; noninvasive; brain mapping; low intensity focused ultrasound; thalamus; somatosensory evoked potentials

Corresponding Author: Robert F. Dallapiazza, MD PhD, University of Virginia, School of Medicine, Department of Neurosurgery, PO Box 800212, Charlottesville, Virginia 22908, Phone: (434) 924-3422, Fax: (434) 982-3806, rd4pm@virginia.edu.

INTRODUCTION:

Acoustic energy has long been known to influence the activity of electrically-excitable tissues including muscle, peripheral nerves, and the central nervous system.[1,12,14,15] During the 1950s, high intensity focused ultrasound was used experimentally to reversibly inhibit neuronal activity by moderate heating below the threshold for tissue ablation,[13] and it was used clinically to treat patients with movement disorders and brain tumors.[16,27]

Advances in noninvasive, transcranial delivery of ultrasound over the past 15 years have renewed an interest in its use for neurosurgical applications.[3–6,17,18,28] Transcranial high intensity focused ultrasound (HIFU) can be delivered in a precise, highly localized manner with millimeter accuracy to induce tissue ablation in deep cerebral structures in the human brain. The clinical effects of HIFU therapy have been highlighted in several recent clinical trials among patients with movement disorders and psychiatric diseases.[2,9,19,25,26]

Perhaps the most exciting, yet largely unharnessed, potential for transcranial ultrasound is for neuromodulation and noninvasive brain mapping with low intensity focused ultrasound (LIFU). The mechanisms of LIFU are non-thermal, and are thought to be mediated by mechanical forces within the brain tissue.[31,32] LIFU shares many of the appealing characteristics of HIFU. It can be focused through the human skull to target deep cerebral structures without affecting intervening tissues, while demonstrating a high spatial accuracy that is not available with current noninvasive neuromodulation methods such as transcranial magnetic stimulation or transcranial electrical stimulation.

Most current studies of LIFU neuromodulation have applied ultrasound to the motor cortex of rodents in order to elicit muscle contractions.[20,21,29,33,34] Limb, tail, whisker, and eye muscles can be independently activated depending on the LIFU focus. However, somatotopic mapping is difficult due to the mismatch in the size between the acoustic focus and the rodent brain.[21] More recently, Legon et al and Lee et al applied LIFU to the human somatosensory cortex, demonstrating that ultrasound could suppress median nerve evoked potentials on EEG and stimulate subjective somatosensory phenomenon.[22,24]

Despite these exciting advances, there remains a need for a large animal brain model of LIFU neuromodulation.[8,23] Furthermore, previous work with LIFU does not fully highlight the capabilities of LIFU neuromodulation; namely, its ability to noninvasively penetrate deep cortical structures (beyond the cerebral cortex) with a high spatial resolution (millimeter scale). In this article, we describe a large-brain animal model that targets LIFU to the somatosensory thalamus, alters somatosensory evoked potentials for long durations, is selective and precise within 2 mm, and does not result in tissue heating or histological damage.

MATERIALS AND METHODS:

Anesthesia and surgery:

Anesthesia was induced with a single intramuscular injection of Telazol (6mg/kg) and xylazine (2mg/kg). The animals were moved from the cage area to a surgical preparation

room. An intravenous catheter was place in the marginal vein of each ear. An endotracheal tube was placed and secured to the mandible. Anesthesia was maintained with a continuous infusion of propofol at 10mg/kg/hr. Animals were placed on a ventilator 10ml/kg tidal volume at a rate of 18 breaths/minute of room air. Prior to SSEP testing, animals were started on an IV drip of rocuronium (200mg diluted in a 500ml bag of normal saline). The drip rate was set to administer 2.0–2.5mg/kg/hr. The effects of paralytics were assessed using physical indicators such as palpebral reflex, eye position, toe pinch, and jaw tone. Depth of anesthesia and analgesia were monitored by continuous measurements of heart rate and oxygen saturation.

To implant the epidural electrode, the scalp was first infiltrated with 0.25% marcaine, and then a U-shaped incision was made to reflect the scalp posteriorly. A 4 × 4 cm craniectomy centered on the bregma was performed using a high speed drill, and the dura matter was kept intact. A four contact epidural recording electrode was placed over the right cerebral hemisphere and tucked laterally out of the ultrasonic beam path. The electrode was secured to the dura and tunnel posteriorly for electrophysiological recordings.

Electrophysiology and somatosensory evoked potentials:

A thirty-two channel recording system with 9 channels for stimulation was used to measure SSEPs in swine (Cadwell Cascade Pro, Kennewick, WA). MR-compatible platinum electrodes (Genuine Grass F-E2–24) were used for bipolar stimulation of the trigeminal (snout), median (forelimb), and tibial (hindlimb) nerves. Recording electrodes were placed midline at the front of the skull, midline at the back of the skull, 4cm laterally in each direction from midline at the back of the skull, over the cervical spine, and bilaterally over the brachial plexus in the shoulder. A 1X4 cortical grid was implanted over the right lateral convexity of the cortex to optimize recordings. All recordings were referenced to a cephalic recording electrode with the exception of the brachial plexus electrodes, which were referenced to each other.

Peripheral stimulation frequency ranged between 2–3 Hz, and stimulation amplitude varied from 12 to 15 mA with 0.3 msec square wave pulse duration. Fifty to three hundred trials were averaged, and stable baseline recordings were obtained for 10 to 20 minutes prior to ultrasound exposure. The trigeminal nerve cortical response was typically observed 12–13 msec after the stimulation artifact, the median nerve cortical response was 14–16 msec after the stimulation artifact, and the tibial nerve cortical response was 16–18 msec after the stimulation artifact.

MR-guided focused ultrasound

Ultrasound Pulsing Protocol: All neuromodulation experiments (LIFU sonications) were performed at 25–30 W/cm^2 (ISA), with a pulse duration of 43.7 msec and a pulse repetition time of 100 msec (duty cycle= 43.7%, Fig. 1c). The sonication duration was 40 seconds in total. In all studies, the animal was coupled to the transducer by a degassed water bath. HIFU sonications were performed by applying continuous-wave power at 20W for 20s and were used to verify targeting and MR thermometry results. These HIFU sonications were

performed only after all neuromodulation LIFU sonications had been completed in the animal.

Preclinical 1.14 MHz FUS System: This device (RK-100, FUS Instruments, Inc.) utilizes a single-element spherically focused transducer powered by a 50 dB amplifier and driven by a function generator (33210A, Agilent) at 1.145 MHz. The focal region is approximately 1.5 × 1.5 × 7.5 mm. The device uses a motor-controlled 3-axis positioning system to adjust the location of the acoustic focus, with sub-mm accuracy.

Clinical 3T MRI scanner: The pre-clinical 1.14 MHz FUS system was placed on the patient table of a whole-body 3T MRI scanner (Trio, Siemens Medical Solutions). Before positioning the animal on the FUS platform, the coordinate systems of the FUS and MRI systems were synchronized by using MR thermometry to locate a HIFU-induced focal temperature rise in an anechoic Zerdine phantom (CIRS, Inc). The animal was then positioned supine on the FUS platform with its brain directly above the upward-facing transducer. The patient table was slid into the magnet bore, and T2-weighted fast spin-echo images of the brain were acquired. These images were used to identify the desired thalamic targets and determine their spatial coordinates. The patient table was then slid all the way out of the magnet bore to prepare for the SSEP measurements of LIFU sonications.

Clinical 710 and 220 kHz FUS systems: Ultrasound experiments at 650 and 220 kHz were performed in a similar manner using the clinical ExAblate Neuro (InSightec; Haifa, Israel) coupled to a 3 T MRI system (Discovery MR750, GE Healthcare). The 650 kHz transducer consists of a hemispherical (30 cm diameter) 1024-element phased array transducer with approximately a 4 × 4 × 6 mm focal region and 0.72 mm accuracy. The 220 kHz transducer consists of a hemispherical (30 cm diameter) 990-element phased array transducer with a 4 × 4 × 6 mm focal region and 0.72 mm accuracy.

Magnetic resonance thermography:

MR thermography was performed in each animal during separate HIFU and/or LIFU sonications, after all SSEP measurements had been completed. Temperature was monitored in a single slice through the ultrasound focus, by acquiring a time series of temperature-sensitive gradient-echo MR images beginning before the start and continuing beyond the end of each sonication period, using the following MR parameters: slice thickness= 3 mm, flip angle= 25°, repetition time (TR)= 39 ms, echo time (TE)= 10 msec, field of view= 250 mm, matrix= 256 × 256, readout bandwidth = 80 Hz/pixel, acquisition time = 5 s/image. Maps of temperature change relative to pre-sonication baseline were calculated from the resulting phase images using the standard proton-resonance-frequency shift method [31], and maps of absolute temperature versus time were constructed assuming a baseline body temperature of 39°C.

Theoretical computational temperature increases with low and high intensity ultrasound:

The theoretical temperature rise was calculated using the HIFU Simulator V1.2, which first integrates the axisymmetric Khokhlov–Zabolotskaya–Kuznetzov (KZK) equation from the frequency-domain and then inputs the temporal average intensity and heating rate into the bioheat transfer (BHT) equation to determine the temperature rise at the focus and the total

thermal dose delivered. The parameters used in the simulations are available in Tables 1 and 2. Sonication parameters and beam path geometry were determined from experimental settings, and tissue properties for human grey matter were collected from published data (Table 1 and 2). Resolution was adjusted to 1 mm to match the resolution of MR thermography images.

Histology:

Animals were euthanized with a lethal overdose of barbiturates, and whole brains were immediately dissected and placed in 10% formalin. Brains were fixed for at least 14 days prior to sectioning. Once fixation was complete, the brains were sectioned in ~3 mm blocks in the coronal plane. The ventrolateral thalamic nucleus was identified and removed en bloc and placed in cassettes. Tissues were embedded in paraffin wax and cut in 5 μm sections. Serial sections were cut every 100 μm and stained with hematoxylin and eosin or luxol fast blue. Gross and microscopic evaluations were performed with a certified neuropathologist.

RESULTS:

Thalamic neuromodulation with LIFU:

We first sought to determine whether LIFU could temporarily suppress the activity of thalamocortical relay neurons in the ventroposterolateral thalamic nucleus (VPL). In anesthetized swine, SSEPs were obtained by stimulating the left median nerve and recording the evoked cortical responses with an epidural electrode implanted over the right lateral convexity of the cortex. The thalamus was imaged with 3 Tesla MRI, and the VPL was located with the aid of a stereotactic swine brain atlas.[11] The acoustic focus from a single-element, MR-compatible 1.14 MHz focused US transducer (1.5 mm FWHM laterally, 7.5 mm FWHM axially, and 5.7 cm focal distance, Figure 1) was stereotactically aligned to the VPL (Figure 2a and 2b). Acoustic energy was delivered with the following parameters: 43. 7 msec pulse duration, 10 Hz pulse repetition frequency, and 40 second total sonication duration. The spatial acoustic intensity was 25W/cm^2, and the mechanical index was 0.53 (Figure 1c).

LIFU delivered to the right VPL decreased left median nerve SSEPs to 71.6 ± 11.4 % compared to baseline recordings (Figures 2c and 2d). Contralateral control sonications in the left VPL had little effect on left median nerve SSEPs (96.3 ± 7.3 % of baseline values at 5 min post sonication; Figures 1c and 1d). Peak electrophysiological suppression was seen 5 minutes after acoustic exposure and returned to near baseline values within 20 minutes (Figures 2c and 2d). HIFU ablations in the VPL resulted in permanent loss of SSEPs (Supplemental Figure 1).

Thalamic mapping with LIFU neuromodulation:

Since the acoustic focus of the 1.14 MHz experimental ultrasound transducer and the 710- and 220 kHz clinical ultrasound transducers (Insightec, LTD; Haifa, Israel) were small enough to target a single thalamic nucleus in the swine brain, we next sought to determine whether LIFU neuromodulation could be used to noninvasively map the ventrolateral thalamic nuclear complex using the experimental (N = 2) and clinical (N =2) ultrasound

transducers. Like the somatotopic organization of the sensory cortex, the ventrolateral thalamic nuclear complex has a distinct somatotopic organization with trigeminal (snout) inputs synapsing in the ventroposteromedial (VPM) nucleus and somatic (median and tibial nerves) inputs synapsing in the ventroposterolateral (VPL) nucleus. These nuclei are functionally distinct, but are indistinguishable on high resolution MR imaging, and histologically they form a continuum without clear borders.

To determine the spatial resolution of LIFU, we first sonicated a region of the thalamus 2 mm anterior to the ventrolateral thalamic nuclear complex (Fig. 3a) with LIFU while recording evoked potentials from the trigeminal (snout) and tibial (hindlimb) nerves in sequence (Fig. 3b). During this “off-target,” control sonication, there were no significant changes in either the trigeminal-evoked or tibial-evoked cortical potentials compared to baseline recordings (trigeminal, 98.2 ± 4.5 % and tibial, 100.6 ± 4.4 %; $p = 0.40$ and 0.42, respectively)(Fig. 3c and 3d, N = 5 sonications, 4 animals). Next, we adjusted the acoustic focus to target the right VPM (Fig 3e). LIFU sonication of the VPM resulted in a decrease in trigeminal-evoked cortical potentials to 76.9 ± 7.5 % of baseline values (N = 6 sonications, 4 animals; $p = 0.0002$), and tibial-evoked potentials were not significantly changed at 102.0 ± 4.3 % compared to baseline values (N = 6 sonications, 4 animals; $p = 0.19$)(Fig. 3f, 3g, and 3h). Then the acoustic focus was aligned with the right VPL (Fig. 4i). LIFU sonication of the VPL had no significant effect on trigeminal-evoked cortical potentials (103.9 ± 3.3 %, $p > 0.05$), however tibial-evoked potentials decreased significantly to 83.9 ± 4.3 % compared to baseline values (N = 6 sonications, 4 animals, $p = 4.2 \times 10^{-6}$)(Fig 3j, 3k, and 3l).

Temperature monitoring during LIFU:

Next, we sought to determine whether the LIFU parameters used for thalamic neuromodulation caused tissue heating at the acoustic focus. We used two-dimensional, proton-resonance shift MR thermography to image the acoustic focus and measure tissue heating during LIFU and HIFU sonications.[7] During LIFU sonications (N = 4) there were no observable temperature increases at the acoustic focus in comparison to background signal noise with a sensitivity < 5 °C (Fig. 4b). Post LIFU T2*-weighted imaging did not show any signal change at the focus (Fig. 4a). During HIFU sonications (20 W, 20 sec; N = 6), peak voxel temperatures increased by 25–50 °C (Fig 4e), and post HIFU T2*-weighted images demonstrated a small area of increased signal at the acoustic focus corresponding to tissue ablation (Fig. 4f).

To further determine whether LIFU sonications subtly increased tissue temperature that was below the sensitivity of standard MR thermography, we performed a series of experiments using increasing sonication duration and intensity. Using the same ultrasound parameters described in Fig. 1c, we increased the total sonication duration six-fold (240 sec) to allow for increased MR averaging and improved signal-to-noise ratios. During this sonication, average temperatures were −0.1 ± 0.3 °C compared to baseline temperatures (Fig. 4c). Next, we systematically increased the sonication energy from 0.25 W to 16 W. There were no observable temperature increases with sonication intensities ranging from 0.25 – 2 W. Sonication at 4 W, a 16-fold increase in power, resulted in a ~3 °C thermal rise at the acoustic focus (Fig 4d).

We used the HIFU Simulator V1.2 to predict temperature changes based on our sonication parameters. Sonication parameters and beam path geometry were determined based on experimental settings, and tissue properties for human grey matter were collected from published data (Supplemental Table 1 and 2). Resolution was adjusted to 1 mm to match the resolution of MR thermography images. For LIFU sonications, the predicted thermal rise at the focus was 0.13 °C (Fig. 4g), which agrees with our measured thermal rise of 0.1 ± 0.3 °C. The predicted temperature rose steadily throughout the sonication, reaching peak at 40 sec, and returned to baseline in 25 sec (Fig. 4g). The predicted volume of tissue exposed to an increase in temperature of more than 0.05 degrees was 1 × 1× 3 mm, which is in agreement with the dimensions of the acoustic focus (Fig. 4h).

Histological analysis:

Gross and microscopic histological analysis were performed in all animals (N = 10). Eight animals received LIFU targeting the right ventrolateral thalamus (Fig. 5a), and six animals received HIFU targeting the left thalamus (Fig. 5e). Fixed whole brains were cut in the coronal plane, and the ventrolateral thalamic nucleus was identified grossly. Among the animals that received LIFU in the right ventrolateral thalamus, there was no gross evidence of tissue damage. In animals that received HIFU in the left thalamus, lesions were identified in all animals and varied in appearance from dark discoloration without overt tissue disruption to well-circumscribed lesions with surrounding tissue edema, which correlated to the peak temperature observed during MR thermography. Serial sections were stained with hematoxylin/eosin (HE) and Luxol Fast Blue (LFB). In sections from animals treated with LIFU there was no microscopic evidence of tissue damage. Neurons had a normal appearance, and there was no evidence of disruption of the white matter tracts around the ventrolateral thalamic nuclei (Fig. 5b–d, LFB not shown). These were indistinguishable from control sections that were untreated with ultrasound. In sections from animals treated with HIFU, there was a characteristic necrotic core with cellular debris and tissue disruption.[10] Surrounding the necrotic core there were ischemic neurons and bubbly, edematous changes in the white matter (Fig. 5f–h). Microscopic analysis of the overlying cortex and adjacent white matter tissues within the acoustic path of ultrasound did not show any evidence of tissue disruption.

DISCUSSION:

LIFU for noninvasive neuromodulation and brain mapping:

In these experiments pulsed, low intensity focused ultrasound was targeted to the ventrolateral thalamus in swine resulting in reversible suppression of somatosensory evoked cortical potentials by 20–50%. Given the high spatial resolution of focused ultrasound, we were able to selectively target the sub-nuclei within the somatosensory thalamus. Thus, we were able to selectively suppress evoked potentials through the trigeminal system by targeting the ventroposteromedial nucleus while leaving the lemniscal pathways that synapse in the ventroposterolateral nucleus unaltered. Furthermore, focused ultrasound targeted as little as 2 mm anterior to the ventrolateral thalamus had no effect on evoked potentials.

Prior studies examining the effects of low intensity ultrasound in the brain have had limited success in demonstrating anatomic specificity. Among rodent studies, a variety of motor responses have been elicited by ultrasound focused on the motor cortex. However, a somatomotor map has been difficult to assess secondary to a mismatch in the size of the acoustic focus and the size of the rodent brain.[21,29,30,34] In human studies, Legon et al found that ultrasound targeting the post-central gyrus could inhibit median-nerve evoked potentials, and translational movements of the transducer 5 mm from the post-central gyrus had no effect.[24] However, this study did not examine whether lateral movements along the post-central gyrus, corresponding to facial representation, could inhibit somatosensory evoked potentials from the trigeminal system.

Current studies of low intensity ultrasound neuromodulation in large-brain animal models and humans have used short ultrasound pulses targeting the cerebral cortex. Deffieux et al targeted the frontal eye fields (Broadman's Area 8) in awake nonhuman primates and demonstrated an impairment in antisaccadic eye movements.[8] Legon et al also used short ultrasound pulses targeting somatosensory cortex in concurrence with median nerve stimulation to demonstrate decreased evoked potential amplitudes recorded by EEG.[24] In each of these studies, ultrasound impaired short-term neural function during brief tasks or recording procedures with rapid recovery on subsequent trials. We found that longer ultrasound pulses delivered over prolonged periods of time resulted in a substantial and sustained decrease in neural function that lasted for a period of several minutes, but caused no lasting damage.

LIFU safety:

The Food and Drug Administration regulates the safety of diagnostic ultrasound devices, and several therapeutic devices have investigational approval. Given the wide array of applications and device variability, there are several recommended safety metrics including spatial- and time-averaged intensities, and mechanical and thermal indices for diagnostic devices. These metrics can vary widely based on the acoustic frequency, acoustic power, duration of exposure, and pulsing schemes. Ultimately, the safety of low intensity focused ultrasound devices will need to be determined in animal models or in computational models.

We monitored tissue temperature at the acoustic focus during LIFU sonications using proton-shift magnetic resonance and found no heating above the sensitivity measurements (< 1 °C). In addition, we applied the ultrasound parameters used for neuromodulation into HIFU simulation software and determined that theoretical temperature increases from these parameters would result in < 1 °C heating. These results suggest that the ultrasound parameters used in this study are unlikely to significantly heat tissues and can safely be applied for human use.

Mechanism of LIFU neuromodulation:

The precise mechanisms of neuromodulation with ultrasound are incompletely understood. At higher intensities, focused ultrasound causes tissue heating and cavitation by generating frictional energy and low pressure fields at the acoustic focus that can reversibly impair neural function. With low intensity focused ultrasound, tissue heating and cavitation are less

likely mechanisms. Focused ultrasound also exerts a mechanical force as pressure waves move through tissues.[31] One of the leading hypothesis for low intensity ultrasound neuromodulation is that mechanical energy or intramembrane cavitation impart physiological changes in membrane fluidity and permeability leading to neuronal depolarization. This concept not only applies to the plasma membrane, but also to intracellular membrane compartments such as synaptic vesicles and mitochondria, which rely on electrochemical gradients to properly function. There is already evidence that low intensity ultrasound can alter synaptic vesicle density shortly after exposure.

Mechanical energy from ultrasound could also induce structural changes in transmembrane receptors and voltage-gated ion channels that could lead to their activation or inhibition. Tufail et al demonstrated that pharmacological inhibition of voltage-gated Na^+ and Ca^{2+} channels blocks ultrasound-induced depolarization in both neurons and glia in ex vivo slice experiments.[29] Furthermore, mechanical energy from ultrasound could temporarily disrupt delicately organized synaptic signalosomes within the postsynaptic density. Adrianov et al used electron microscopy to analyze the effects of low intensity ultrasound on the feline lateral geniculate nucleus and found widening of the synaptic cleft and a decrease in the thickness of the postsynaptic density.[1] Given the relative long-lasting effects we observed after LIFU sonication of the ventrolateral thalamus, it is tempting to speculate that prolonged ultrasound exposures could lead to some form of short-term synaptic plasticity. Certainly, further work is necessary to support these claims; however, it bears mentioning since long term neural suppression with ultrasound could potentially have a large impact on noninvasive therapeutic neuromodulation strategies.

Applications of LIFU neuromodulation:

In this study, we adapted two different clinical-grade HIFU ultrasound transducers (ExAblate Neuro; Insightec, Haifa, Israel) to apply low intensity focused ultrasound to the thalamus in swine (Fig. 6). This required calibration of the device for lower intensities and electronic programming to accommodate pulsed (versus continuous) sonications. Thus, currently available HIFU systems can be easily modified to apply pulsed LIFU. LIFU neuromodulation could be used immediately for intraprocedural target confirmation and brain mapping during therapeutic, focused ultrasound ablations. For example, LIFU could be targeted to the thalamic VIM nucleus to verify tremor suppression prior to ablation among patients being treated for essential tremor. It could also be used to map the somatosensory thalamus so that it could be protected during HIFU treatments.

Furthermore, most current HIFU transducers are MR-compatible, and FUS procedures are largely MR-guided. It is conceivable that LIFU neuromodulation could be used in combination with MR-based measurements such as fMRI. This could provide an unparalleled opportunity to study the human brain in a highly localized, noninvasive manner in a variety of neurological diseases and among healthy individuals.

CONCLUSIONS:

In this study, we demonstrate that low intensity focused ultrasound can be used to selectively inhibit thalamic relay neurons in swine with a high spatial resolution. These physiological

effects were observed without evidence of tissue heating or histological damage. Low intensity focused ultrasound is an emerging method for neuromodulation and noninvasive brain mapping and may have a variety of applications in human brain studies and for therapeutic neuromodulation.

Supplementary Material

Refer to Web version on PubMed Central for supplementary material.

Abbreviations:

HIFU	High intensity focused ultrasound
LIFU	Low intensity focused ultrasound
VPL	ventroposterolateral thalamic nucleus
VPM	ventroposteromedial thalamic nucleus
SSEPs	somatosensory evoked potentials
fMRI	functional magnetic resonance imaging

REFERENCES:

1. Adrianov OS, Vykhodtseva NI, Fokin VF, Uranova NA, Avirom VM: [Reversible functional shutdown of the optic tract on exposure to focused ultrasound]. Biull Eksp Biol Med 97:760–762, 1984 [PubMed: 6743822]
2. Chang WS, Jung HH, Kweon EJ, Zadicario E, Rachmilevitch I, Chang JW: Unilateral magnetic resonance guided focused ultrasound thalamotomy for essential tremor: practices and clinicoradiological outcomes. J Neurol Neurosurg Psychiatry 86:257–264, 2015 [PubMed: 24876191]
3. Clement GT, Hynynen K: A non-invasive method for focusing ultrasound through the human skull. Physics in Medicine & Biology 47:1219–1236, 2002 [PubMed: 12030552]
4. Clement GT, Sun J, Giesecke T, Hynynen K: A hemisphere array for non-invasive ultrasound brain therapy and surgery. Phys Med Biol 45:3707–3719, 2000 [PubMed: 11131194]
5. Clement GT, White J, Hynynen K: Investigation of a large-area phased array for focused ultrasound surgery through the skull. Phys Med Biol 45:1071–1083., 2000 [PubMed: 10795992]
6. Clement GT, White PJ, King RL, McDannold N, Hynynen K: A magnetic resonance imaging-compatible, large-scale array for trans-skull ultrasound surgery and therapy. Journal of Ultrasound in Medicine 24:1117–1125, 2005 [PubMed: 16040827]
7. De Poorter J, De Wagter C, De Deene Y, Thomsen C, Stahlberg F, Achten E: Noninvasive MRI thermometry with the proton resonance frequency (PRF) method: in vivo results in human muscle. Magn Reson Med 33:74–81, 1995 [PubMed: 7891538]
8. Deffieux T, Younan Y, Wattiez N, Tanter M, Pouget P, Aubry JF: Low-intensity focused ultrasound modulates monkey visuomotor behavior. Curr Biol 23:2430–2433, 2013 [PubMed: 24239121]
9. Elias WJ, Khaled M, Hilliard JD, Aubry JF, Frysinger RC, Sheehan JP, et al.: A magnetic resonance imaging, histological, and dose modeling comparison of focused ultrasound, radiofrequency, and Gamma Knife radiosurgery lesions in swine thalamus. J Neurosurg 119:307–317 [PubMed: 23746105]
10. Elias WJ, Khaled M, Hilliard JD, Aubry JF, Frysinger RC, Sheehan JP, et al.: A magnetic resonance imaging, histological, and dose modeling comparison of focused ultrasound,

radiofrequency, and Gamma Knife radiosurgery lesions in swine thalamus. J Neurosurg 119:307–317, 2013 [PubMed: 23746105]

11. Felix B, Leger ME, Albe-Fessard D, Marcilloux JC, Rampin O, Laplace JP: Stereotaxic atlas of the pig brain. Brain Res Bull 49:1–137, 1999 [PubMed: 10466025]
12. Foley JL, Little JW, Vaezy S: Image-guided high-intensity focused ultrasound for conduction block of peripheral nerves. Ann Biomed Eng 35:109–119, 2007 [PubMed: 17072498]
13. Fry FJ, Ades HW, Fry WJ: Production of reversible changes in the central nervous system by ultrasound. Science 127:83–84, 1958 [PubMed: 13495483]
14. Gavrilov LR: Use of focused ultrasound for stimulation of nerve structures. Ultrasonics 22:132–138, 1984 [PubMed: 6372189]
15. Harvey: The effect of high frequency sound waves on heart muscle and other irritable tissues. Am J Physiology 91:284–290, 1929
16. Heimburger RF: Ultrasound augmentation of central nervous system tumor therapy. Indiana Med 78:469–476, 1985 [PubMed: 4020091]
17. Hynynen K, McDannold N, Clement G, Jolesz FA, Zadicario E, Killiany R, et al.: Pre-clinical testing of a phased array ultrasound system for MRI-guided noninvasive surgery of the brain--a primate study. European Journal of Radiology 59:149–156, 2006 [PubMed: 16716552]
18. Ishihara Y, Calderon A, Watanabe H, Okamoto K, Suzuki Y, Kuroda K, et al.: A precise and fast temperature mapping using water proton chemical shift. Magn Reson Med 34:814–823, 1995 [PubMed: 8598808]
19. Jeanmonod D, Werner B, Morel A, Michels L, Zadicario E, Schiff G, et al.: Transcranial magnetic resonance imaging-guided focused ultrasound: noninvasive central lateral thalamotomy for chronic neuropathic pain. Neurosurg Focus 32:E1, 2012
20. King RL, Brown JR, Pauly KB: Localization of ultrasound-induced in vivo neurostimulation in the mouse model. Ultrasound Med Biol 40:1512–1522, 2014 [PubMed: 24642220]
21. King RL, Brown JR, Pauly KB: Localization of ultrasound-induced in vivo neurostimulation in the mouse model. Ultrasound Med Biol 40:1512–1522
22. Lee W, Kim H, Jung Y, Song IU, Chung YA, Yoo SS: Image-guided transcranial focused ultrasound stimulates human primary somatosensory cortex. Sci Rep 5:8743, 2015 [PubMed: 25735418]
23. Lee W, Lee SD, Park MY, Foley L, Purcell-Estabrook E, Kim H, et al.: Image-Guided Focused Ultrasound-Mediated Regional Brain Stimulation in Sheep. Ultrasound Med Biol 42:459–470, 2016 [PubMed: 26525652]
24. Legon W, Sato TF, Opitz A, Mueller J, Barbour A, Williams A, et al.: Transcranial focused ultrasound modulates the activity of primary somatosensory cortex in humans. Nat Neurosci 17:322–329 [PubMed: 24413698]
25. Lipsman N, Schwartz ML, Huang Y, Lee L, Sankar T, Chapman M, et al.: MR-guided focused ultrasound thalamotomy for essential tremor: a proof-of-concept study. Lancet Neurol 12:462–468, 2013 [PubMed: 23523144]
26. Magara A, Buhler R, Moser D, Kowalski M, Pourtehrani P, Jeanmonod D: First experience with MR-guided focused ultrasound in the treatment of Parkinson's disease. J Ther Ultrasound 2:11, 2014 [PubMed: 25512869]
27. Meyers R, Fry WJ, Fry FJ, Dreyer LL, Schultz OF, Noyes RF: Early experiences with ultrasonic irradiation of the pallidofugal and nigral complexes in hyperkinetic and hypertonic disorders. J Neurosurg 16:32–54, 1959 [PubMed: 13621264]
28. Pinton G, Aubry JF, Bossy E, Muller M, Pernot M, Tanter M: Attenuation, scattering, and absorption of ultrasound in the skull bone. Med Phys 39:299–307, 2012 [PubMed: 22225300]
29. Tufail Y, Matyushov A, Baldwin N, Tauchmann ML, Georges J, Yoshihiro A, et al.: Transcranial pulsed ultrasound stimulates intact brain circuits. Neuron 66:681–694, 2010 [PubMed: 20547127]
30. Tufail Y, Yoshihiro A, Pati S, Li MM, Tyler WJ: Ultrasonic neuromodulation by brain stimulation with transcranial ultrasound. Nat Protec 6:1453–1470
31. Tyler WJ: Noninvasive neuromodulation with ultrasound? A continuum mechanics hypothesis. Neuroscientist 17:25–36 [PubMed: 20103504]

32. Tyler WJ, Tufail Y, Finsterwald M, Tauchmann ML, Olson EJ, Majestic C: Remote excitation of neuronal circuits using low-intensity, low-frequency ultrasound. PLoS One 3:e3511, 2008 [PubMed: 18958151]

33. Yoo SS, Bystritsky A, Lee JH, Zhang Y, Fischer K, Min BK, et al.: Focused ultrasound modulates region-specific brain activity. Neuroimage 56:1267–1275

34. Younan Y, Deffieux T, Larrat B, Fink M, Tanter M, Aubry JF: Influence of the pressure field distribution in transcranial ultrasonic neurostimulation. Med Phys 40:082902, 2013 [PubMed: 23927357]

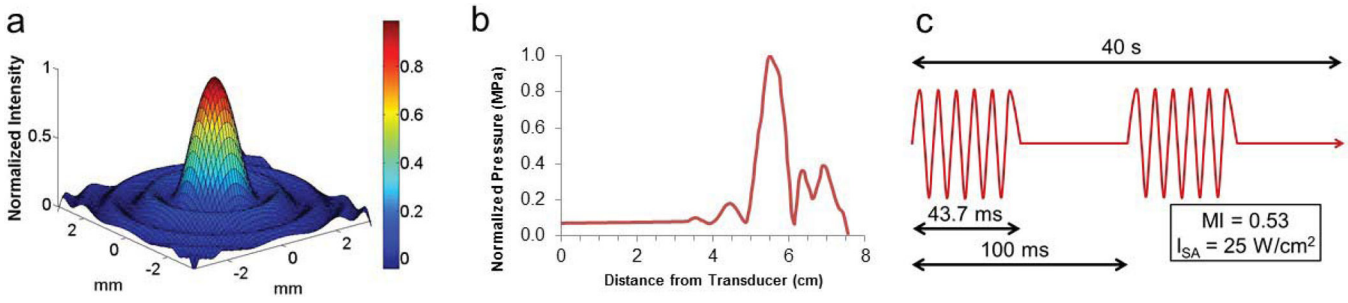

Figure 1.

Ultrasound parameters and characterization. **(a)** The single element 1.14 MHz focused transducer has a narrow 1 × 1 mm focus in the lateral dimension **(b)** and a 5 mm focus in the axial direction, with a focal length of 5.6 cm. **(c)** Neuromodulation treatments were performed with a 43. 7% duty cycle over 40 seconds, with an I_{SA} of 25–30 W/cm^2 maintained across all three (1.14 MHz, 650 kHz, 220 kHz) ultrasound systems used.

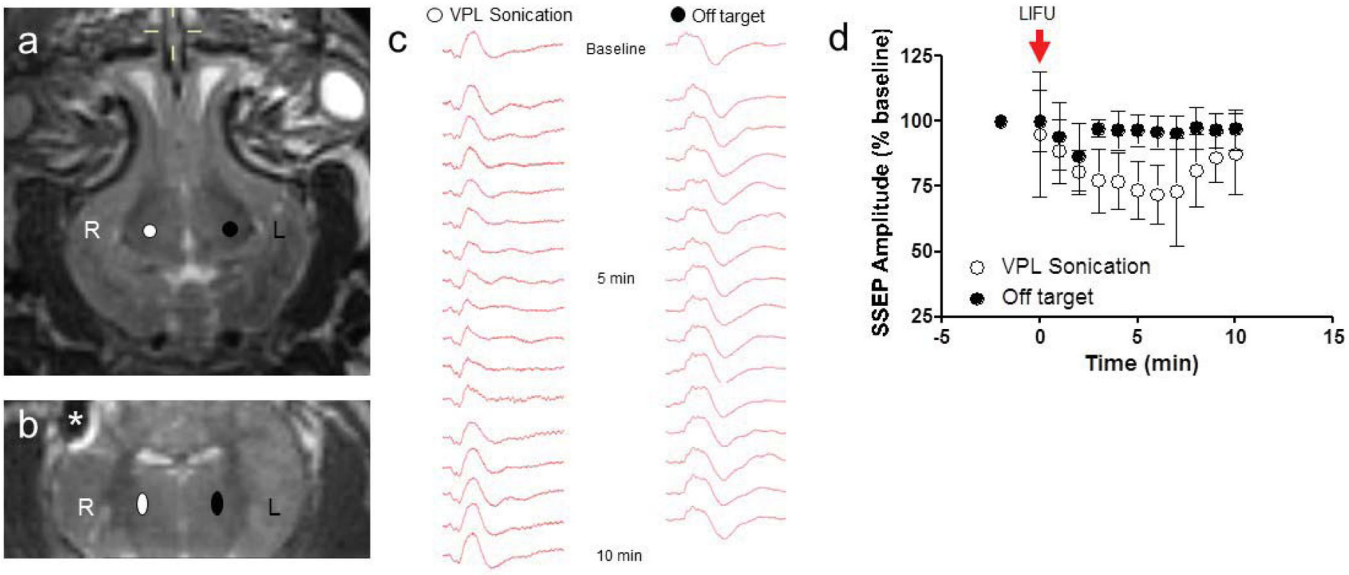

Figure 2.

Thalamic neuromodulation with LIFU. **(a, b)** Axial and coronal T2-weighted MRI demonstrating the right VPL target (*white*), control left VPL target (*black*), and artifact from the cortical electrode(*). **(c)** Representative median nerve SSEP at baseline, 5 minutes and 10 minutes following right VPL LIFU sonication and control, 'off' target sonications. Note the suppression in SSEPs at 5 minutes after sonication, with a return to baseline by 10 minutes. **(d)** LIFU delivered to the right VPL decreased left median nerve SSEP to 71.6 ± 11.4 % (mean ± SD) compared to baseline recordings (N = 9 sonications, 4 animals). SSEPs recovered to 87.2 ± 15.4 % baseline values within 10 minutes. Control sonications in the left VPL had no lasting effects on left median nerve SSEP, which were 96.3 ± 7.4 % of baseline values (N = 6 sonications, 4 animals).

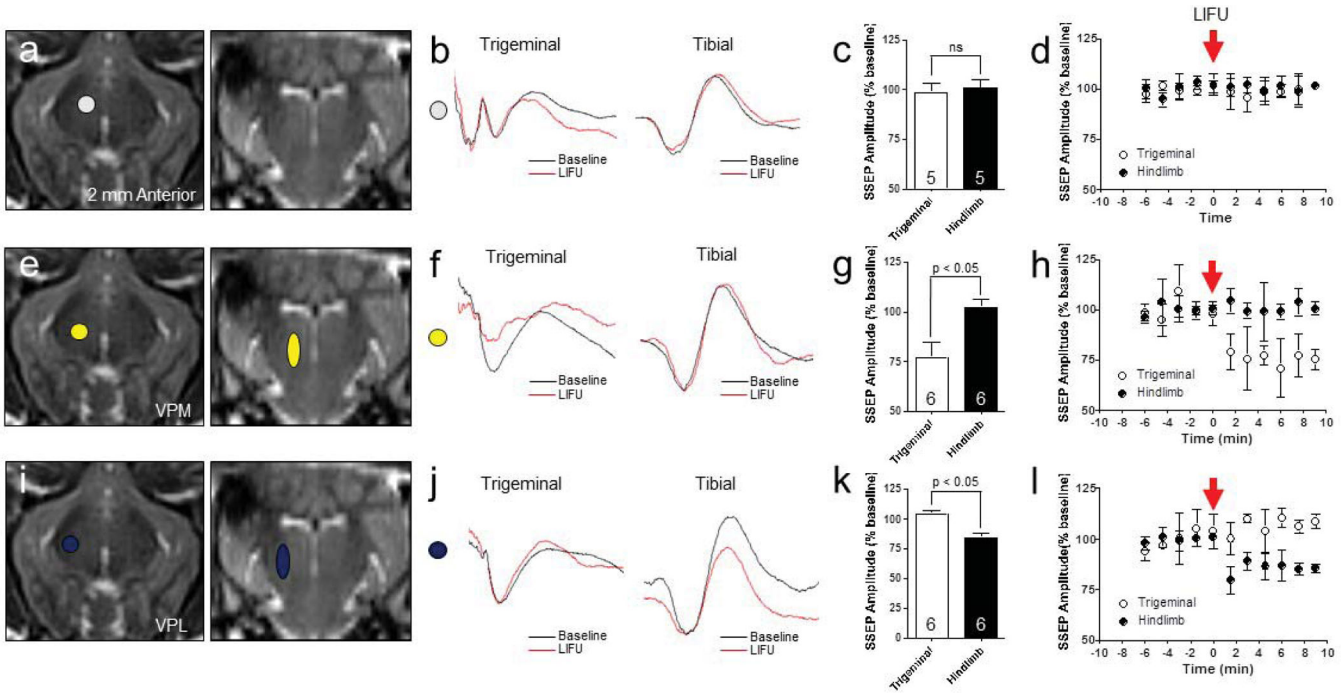

Figure 3.

Noninvasive thalamic nucleus mapping with LIFU. **(a, e, i)** Thalamic nucleus targeting for control (2 mm anterior to VPM, *white shape*), VPM (*yellow shapes*), and VPL (*blue shapes*) with LIFU. **(b, f, j)** Representative trigeminal- and tibial-SSEPs at baseline (*black*) and post-sonication (*red*). **(c, d)** Nontarget, control LIFU did not alter either the trigeminal-evoked or tibial-evoked SSEP compared to baseline recordings (trigeminal, 98.2 ± 4.5 % and tibial, 100.6 ± 4.4 %; p = 0.40 and 0.42, respectively), (N = 5 sonications, 4 animals). The acoustic focus was 2 mm anterior to the VPM target **(g, h)** Right VPM LIFU decreased trigeminal-SSEP to 76.9 ± 7.5 % of baseline values (N = 6 sonications, 4 animals; p = 0.0002), but tibial-SSEP were not significantly changed at 102.0 ± 4.3 % compared to baseline values (N = 6 sonications, 4 animals; p = 0.19). **(k, l)** Right VPL LIFU had no significant effect on trigeminal-SSEP (103.9 ± 3.3 %, p > 0.05), but tibial-SSEP decreased significantly to 83.9 ± 4.3 % compared to baseline values (N = 6 sonications, 4 animals, $p = 4.2 \times 10^{-6}$).

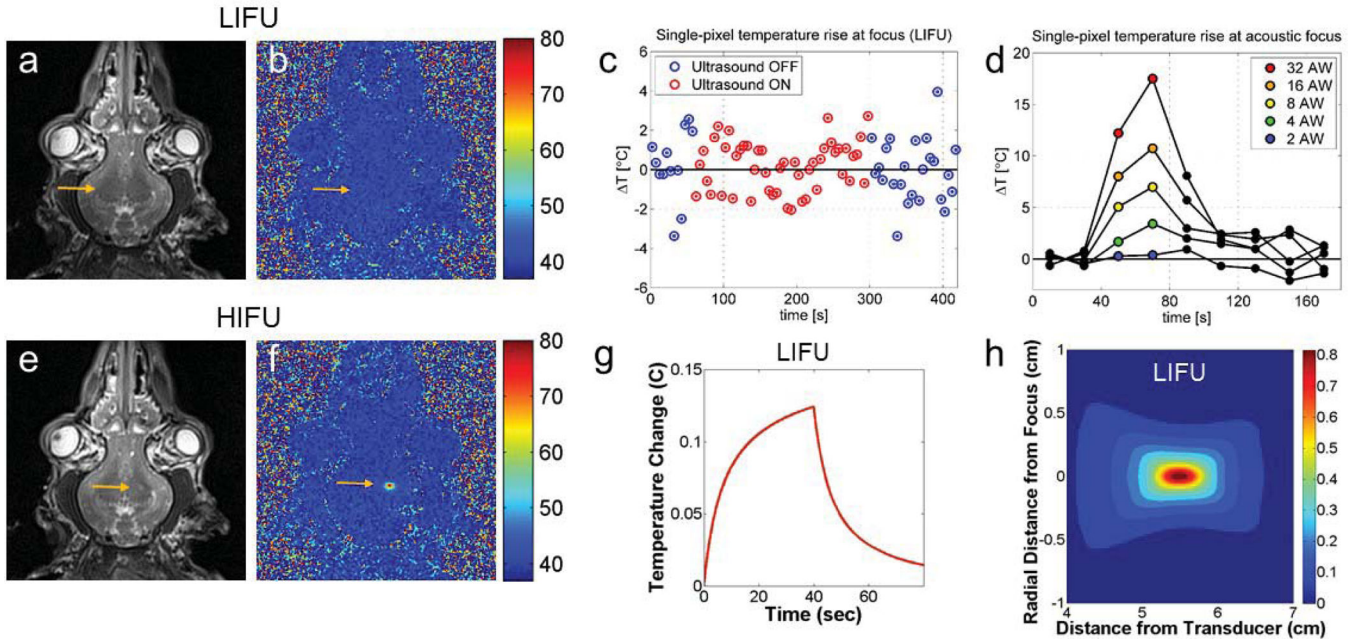

Figure 4.

LIFU temperature monitoring. **(a)** T2-weighted image post LIFU showing no change in signal at the acoustic focus. **(b)** MR proton shift resonance image showing no change in temperature during LIFU. **(c)** Temperature changes at the acoustic focus measured every 5 seconds during a LIFU sonication with a 240-second duration showing a 0.1 ± 0.3 °C average temperature change. *Blue points correspond to baseline MR images, and red points correspond to MR images acquired during sonication*. **(d)** Temperature changes with increasing sonication power confirm that there is no temperature increase until the acoustic power is increased by a factor of 16 (from 0.25 Wto 4 W). **(e)** T2*-weighted image after HIFU showing small hyperintensity at the acoustic focus. **(f)** MR proton shift resonance image confirms temperature elevations during HIFU. **(g)** Modeled temperature rise at the acoustic focus during LIFU sonication predicted by the HIFU Simulator V1.2. The predicted peak temperature, 0.13 °C, occurs at sonication termination. **(d)** Modeled thermal map showing predicted peak spatial temperature rise during LIFU with a 1 × 1 × 3 mm focal heating <0.05 °C.

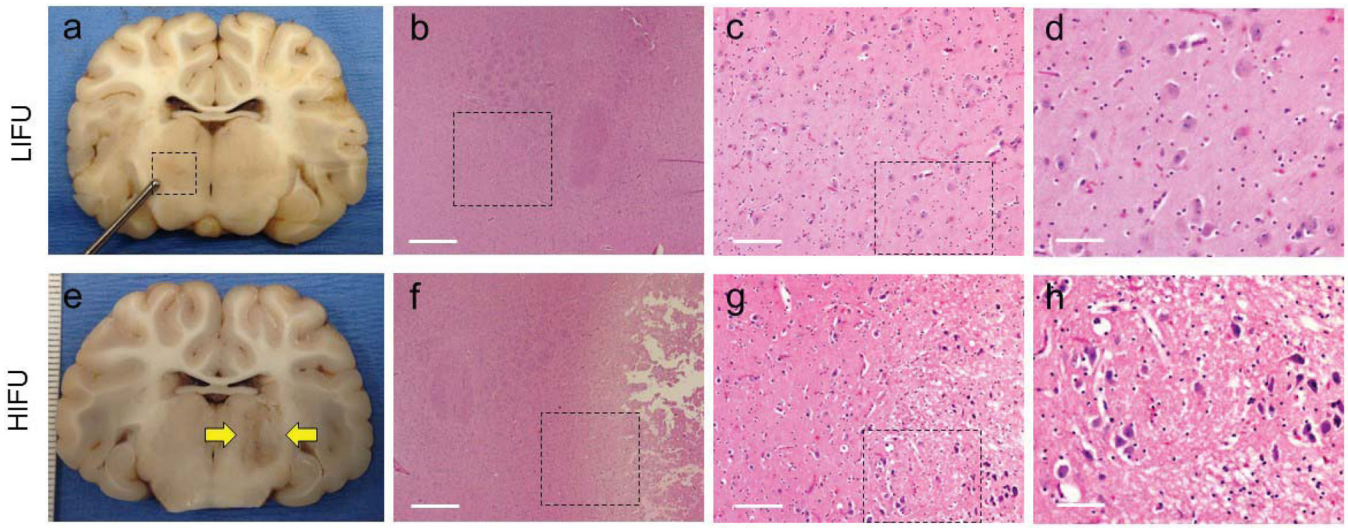

Figure 5.

Gross and histological analysis of thalamic LIFU and HIFU. **(a-d)** LIFU sonications demonstrating no evidence of histological damage. H&E taken at 4×, 10×, and 40×. Black boxes represent the area depicted in the following panel. **(e-h)** HIFU sonication showing well-circumscribed lesion in the ventrolateral thalamus. Microscopic analysis shows ischemic neurons along the periphery and edema extending into the white matter tracts. Black boxes represent the area depicted in the following panel.

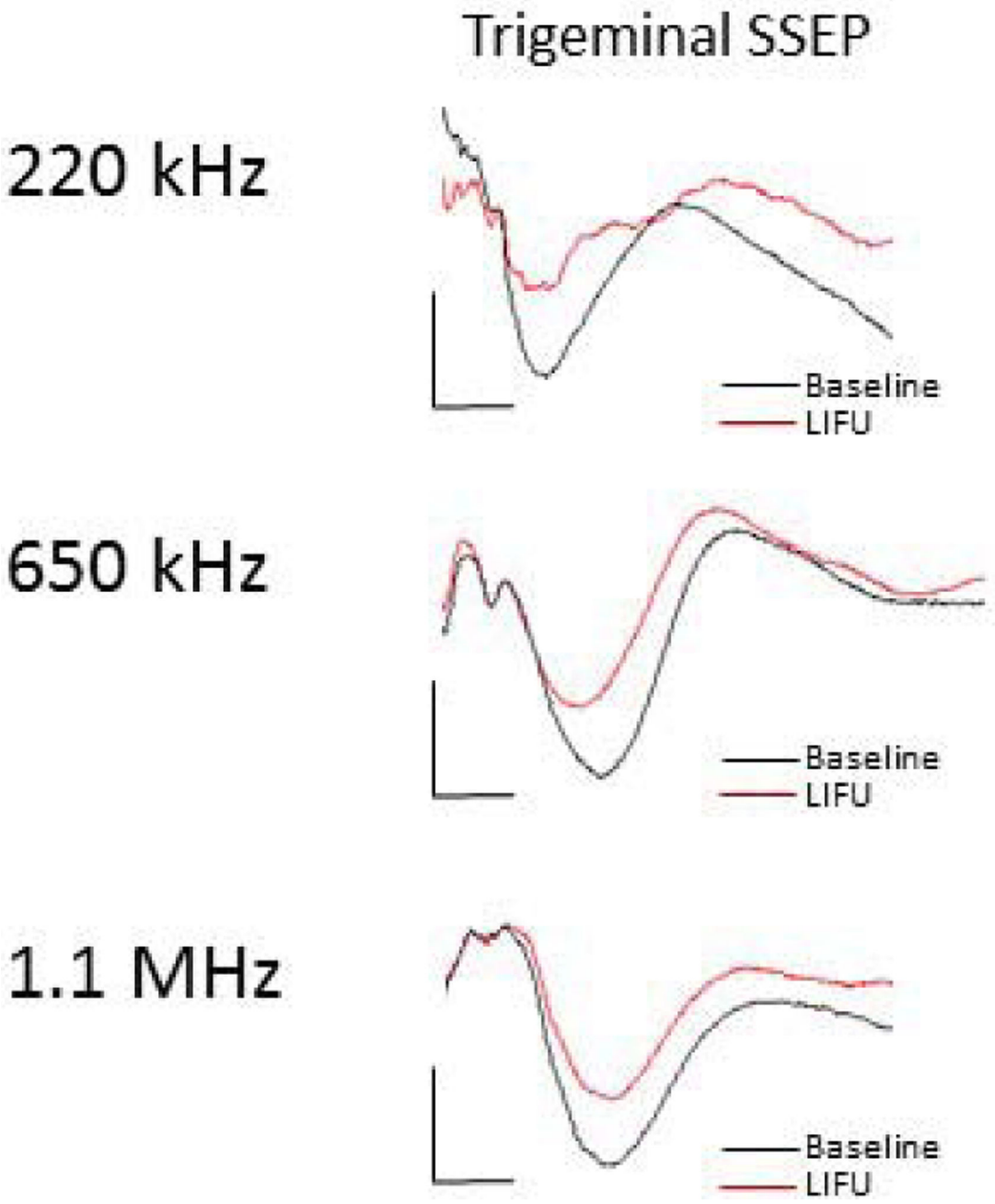

Figure 6.
Thalamic LIFU neuromodulation occurs across ultrasound frequencies. Representative trigeminal-evoked potentials with LIFU focused at the VPM nucleus demonstrating neuromodulation using three separate ultrasound transducers with parent frequencies 220 kHz, 710 kHz, and 1.1 MHz.

TABLE 1:

Parameters used in the Khokhlov–Zabolotskaya–Kuznetzov (KZK) equation from the frequency-domain.

Material	Parameter	Value	Units
Water	speed of sound	1482	m/s
	mass density	1000	kg/m^3
	absorption at 1 MHz	0.217	dB/m
	exponent of absorption vs. frequency curve	2	-
	nonlinear parameter	3.5	-
	material transition distance	3.1	cm
Grey Matter	speed of sound	1550	m/s
	mass density	1045	kg/m^3
	absorption at 1 MHz	80	dB/m
	exponent of absorption vs. frequency curve	1.35	-
	nonlinear parameter	6.9	-
Transducer	outer radius	3.5	cm
	inner radius	0	cm
	focusing depth	5.6	cm
	frequency	1.14	MHz
	power	0.25	W

TABLE 2:

Parameters used for Bioheat transfer (BHT) equation to determine the temperature rise at the focus and the total thermal dose delivered.

Material	Parameter	Value	Units
Water	heat capacity	4180	J/kg/K
	thermal conductivity	0.6	W/m/K
	perfusion rate	0	$kg/m^3/s$
Grey Matter	heat capacity	3696	J/kg/K
	thermal conductivity	0.55	W/m/K
	perfusion rate	14.1	$kg/m^3/s$
	baseline temperature	37	K
Sonication Sequence	initial sonication duration	0.0437	sec
	number of additional pulse sequences	399	-
	duty factor	43.7	%
	pulse cycle period	0.1	sec
	cool-off duration	5	sec